

Direct mass measurements of proton-rich isotopes of Ge,As,Se and Br

G. F. Lima^{1,4}, A. Lépine-Szily¹, G. Audi², W. Mittig³, M. Chartier^{3,5*}, N.A. Orr⁶,
R. Lichtenthaler¹, J. C. Angélique⁴, J.M.Casandjian³, A. Cunsolo⁷, C. Donzaud⁸, A. Foti⁷,
A. Gillibert⁹, M. Lewitowicz³, S. Lukyanov¹⁰, M. MacCormick⁸, D.J.Morrissey¹¹,
A.N.Ostrowski^{3,12}, B.M.Sherrill¹¹, C. Stephan⁸, T. Suomijarvi⁸, L. Tassan-Got⁸, D. J. Vieira¹³,
A. C. C. Villari³, J. M. Wouters¹³

1. Instituto de Fisica-Universidade de São Paulo, C.P.66318, 05315-970 São Paulo, Brazil
2. CSNSM (IN2P3-CNRS&UPS), Bâtiment 108,91405 Orsay Campus, France,
3. GANIL, Boulevard Henry Becquerel, BP 5027, 14021 Caen Cedex, France
4. FACENS - Faculdade de Engenharia de Sorocaba, Sorocaba, Brazil
5. University of Liverpool, Department of Physics, Liverpool, L69 7ZE, UK.
6. LPC, IN2P3-CNRS, ISMRA et Université de Caen 14050 Caen Cedex, France
7. INFN, Corso Itàlia 57, 95129 Catania, Italy,
8. IPN Orsay, BP1, 91406 Orsay Cedex, France,
9. CEA/DSM/DAPNIA/SPhN, CEN Saclay, 91191 Gif-sur-Yvette, France,
10. LNR, JINR, Dubna, P.O.Box 79, 101000 Moscow, Russia,
11. NSCL, Michigan State University, East Lansing MI, 48824-1321, USA
12. Dept of Physics & Astronomy, University of Edinburgh, Edinburgh, EH9 3JZ UK
13. Los Alamos National Laboratory, Los Alamos NM, 87545, USA

The masses of neutron-deficient nuclei close to the proton drip line are an important input for the rapid proton capture (rp)-process modeling above ^{56}Ni . The measurement of the masses of proton-rich nuclei with $32 \leq Z \leq 35$ has been made using a direct time-of-flight technique. The masses of the nuclides ^{66}As , ^{68}Se and ^{71}Br are reported for the first time, with mass-excesses of -51500(680), -53620(1000) and -57060(570) keV being found. The masses agree well in most cases with the Audi-Wapstra systematics.

PAC Numbers: 21.10.Dr, 27.50.+e

I. INTRODUCTION

Proton-rich nuclei heavier than iron are among the least abundant elements in cosmos. Their synthesis is assumed to occur in the rapid proton-capture (rp) process [1,2], in scenarios of extreme high temperature and pressure ($T \geq 8 \times 10^8 \text{K}$, $\rho \geq 10^4 \text{g} \cdot \text{cm}^{-3}$), such as found in X-ray bursts, X-ray pulsars in binary stellar systems involving a matter-accreting neutron star. The hydrogen and helium burning (rp- and α p-process [3]) taking place on the surface of a neutron star powers these bursts and synthesizes heavier elements along the proton drip line that are incorporated in the crust of the neutron star. The investigation of nucleosynthesis and energy generation in the rp-process [4] depends on nuclear masses, the proton-capture reaction and photo-disintegration rates, as well as β -decay and electron capture rates. The time scale of

the rp-process and the observable time-dependence of X-ray bursts thus depend on the masses of nuclei in the vicinity of the proton drip line above nickel.

The rp-process proceeds along the $N=Z$ line which is close to beta stability for light nuclei, but approaches the proton drip line for heavier nuclei. Typically the proton capture reaction rates are orders of magnitude faster than β^+ -decay rates and the reaction pathway follows a series of fast (p, γ) reactions until the proton capture is inhibited. This happens either by proton decay ($Q_p(Z, N) = S_p(Z + 1, N) \leq 0$) or photo-disintegration ($Q_p(Z, N) \sim 0$). The reaction flow then has to wait for the much slower β^+ -decay and the (Z, N) nucleus is referred to as a "waiting-point". The lifetimes of the waiting-point nuclei determine the speed of nucleosynthesis and the resulting abundances. Whether the relatively long-lived nuclides ^{64}Ge ($T_{1/2} = 63.7\text{s}$), ^{68}Se ($T_{1/2} = 35.5\text{s}$) and ^{72}Kr ($T_{1/2} = 17.2\text{s}$) are waiting-points depends on the masses (which, together with the masses of neighbouring nuclei determine the Q_p and Q_β values) and on the β^+ -decay branching ratios (if β^+ -decay is the most important decay mode compared to others). However, experimental information on masses in this region is scarce and consequently mass-models or mass-systematics are employed in network calculations. Recent studies have begun to map the drip line in this mass region [5–9]. Measuring the masses of key nuclei at or close to the drip line are thus important for the accurate modeling of the rp-process.

Another interesting aspect that may be illuminated by the measurement of masses in this region is related to the strength of proton-neutron interactions related to $T=0$ and $T=1$ proton-neutron pairing [10]. The av-

*on leave from CENBG, Université de Bordeaux, Le Haut Vigneau, BP120, 33175 Gradignan, France

erage interaction between the last proton and neutron (in the same shell), can be calculated from the masses of neighbouring nuclei [11,12]. This is particularly enhanced for $N=Z$ nuclei, reflecting the importance of the Wigner symmetry term which is associated with spin-isospin invariance. To investigate this effect in the fp shell the masses around the $N=Z$ line for nuclei in the $A=60-80$ region are required.

II. EXPERIMENTAL METHOD

The present paper describes the measurement of the masses of proton-rich nuclides with $32 \leq Z \leq 35$ using a direct time-of-flight (TOF) method. The first results from this experiment have already been published [13] and the present work represents a re-analysis of the same data, as explained below. Previously, this technique has concentrated on lighter neutron-rich nuclei [14–16].

The technique involves the measurement of the magnetic rigidity ($B\rho$) and the TOF of ions of mass M and charge state $q = Z$ in an achromatic system with a known flight path L . The mass of the ions can then be deduced from the expression,

$$B\rho = \gamma \frac{M}{q} v = \gamma \frac{M}{q} \frac{L}{TOF} \Rightarrow \frac{M}{q} = \frac{TOF}{L} \frac{B\rho}{\gamma} \quad (1)$$

where the relativistic factor, $\gamma = 1/\sqrt{(1-v^2/c^2)}$ also depends on the TOF . The resolving power that can be achieved depends on the resolution in the measurement of the ($B\rho$) and TOF and in previous experiments was on the order of 10^{-4} .

The nuclei of interest were produced by the reaction of a high-intensity ^{78}Kr beam of 73 MeV/nucleon from the GANIL coupled cyclotrons on a $90 \text{ mg/cm}^2 \text{ natNi}$ production target located between the two superconducting solenoids of the SISSI device [17]. Details of the experimental set-up may be found in ref. [13].

The projectile-like fragments emitted from the production target were selected by the alpha-shaped beam-analysis spectrometer and transported along a double achromatically-tuned beam line leading to the focal plane of the high-resolution energy-loss spectrometer SPEG [18]. The TOF ($\sim 1\mu\text{s}$) of the ions was measured over a flight path of 82m between a fast micro-channel plate (MCP) detector (T_{start}) located at the exit of the α -spectrometer and a silicon detector (T_{stop}) located at the focal plane of SPEG. The magnetic rigidity was determined on an event-by-event basis from the position measurement obtained using a position-sensitive MCP detector [19] located at the dispersive image plane of the SPEG analysing magnet after correcting for the finite spot size measured at the focal plane.

A cooled silicon detector telescope was located at the focal plane of SPEG and consisted of three detectors to measure the energy losses (ΔE_1 50 μm , ΔE_2

150 μm , ΔE_{xy} 163 μm) and one stopping detector (E 4.5 mm) to measure the residual energy. Particle identification was obtained by combining these energy measurements with the time-of-flight information. Restricting events to the central region in the position sensitive element of the telescope ΔE_{xy} eliminated ions scattered from the supports of the preceding detectors and considerably improved the energy and time-of-flight resolution.

Two high efficiency (60%) germanium detectors were placed perpendicular to the beam direction on opposite sides of the Si-telescope vacuum chamber. The absolute efficiencies ($\sim 1.4\%$ at $E_\gamma = 1.33 \text{ MeV}$) were determined using a calibrated ^{152}Eu source.

Production rates of $\sim 6 \times 10^5$ ions/s spread over more than 200 different nuclides were predicted [20,21] with only a very small fraction of these being the proton-rich exotic nuclei of interest. A new purification method [13,22] was thus developed to eliminate many of the reaction products that were not of interest and to reduce the total counting rate to acceptable levels in the detector telescope. A thin layer of Ta deposited on the downstream side of the Ni target was added to favour the production of $Z-1$ charge states for the ions of interest. The purification method is based on the stripping of secondary ions (from $q_1 = Z-1$ to $q_2 = Z$) in a thin mylar foil located between the two dipoles of the α spectrometer with the two dipoles tuned asymmetrically so that $B\rho_1/B\rho_2 = q_2/q_1$ and $B\rho_2 = Mv/q_2$. In this way only ions that closely satisfy this condition are transmitted. The selection of different charge state ratios was made by changing *only* the magnetic rigidity, $B\rho_1$, of the first half of the α spectrometer. In the present experiment the region between $Z = 31$ and 35 was covered.

The position measurements were used to correct the dependence of the TOF on the deviation from the central momentum. In our identification spectra we observe many $A/Z=2.0$ exotic nuclides as well as the even more neutron-deficient nuclides ^{61}Ga , ^{63}Ge , ^{65}As and ^{67}Se . As suggested by the experiments of Blank et al [9] and Pfaff et al [23] no events corresponding to ^{69}Br were observed. Unfortunately the heaviest nuclides with well known masses were observed with fairly low statistics. This is due in part to the production cross sections and partly to the charge state ratio purification method used.

A typical mass spectrum for $Z=33$ fragments is presented in Fig.1. In the upper part of this figure the two-dimensional spectrum of TOF versus $E \cdot TOF^2$ is shown. In the upper left corner of each isotope a small group of events arising from ions of the neighbouring element ($Z+1=34$) with different masses ($A+2$) which were not completely filtered out by the identification selection is seen. In some other runs the contamination arose from $Z-1$ and $A-2$ nuclides which appear in the lower right corner. In each case

the procedure described below was used to eliminate these events. Only about 3% of the neighbouring nuclei appear in the $Z=33$ spectrum. The most intense ones ($^{71,72}\text{Se}$ which affect $^{69,70}\text{As}$) are sufficiently well separated in TOF and can be easily excluded by gating on the main group. For lower A nuclei ($^{66,67,68}\text{As}$) where the separation in TOF is less, the amount of contamination is also much lower and the error introduced by any bias in the gating is negligible when compared with other sources of error (statistical and extrapolation).

The lower part of Fig. 1 is a projection onto the TOF axis, after the gates have been applied. The center of gravity $TOF(Z, A)$ and the standard deviation $\sigma(Z, A)$ for each peak was determined in an iterative manner. The mass resolution defined as $\sigma(Z, A)/Mc^2$ was found to be 2×10^{-4} for the most intense peaks. The statistical uncertainty of the TOF is given by $\sigma(Z, A)/\sqrt{N(Z, A)}$ where $N(Z, A)$ is the number of counts in the peak.

It was found that some further precautions had to be taken in the analysis. We observed that the changes in the magnetic rigidity, $B\rho_1$, of the first half of the α -spectrometer had the unexpected effect of also producing slight changes in the TOF and in the energy of the transmitted ions, even though $B\rho_2$ remained unchanged. Thus, accumulating data with different $B\rho_1$ values degraded the energy and TOF resolution. Some species were measured several times with slightly different $B\rho_1$ values. In the present analysis each $B\rho_1$ setting was analysed separately. This resulted in a factor of 3 improvement in precision over the previous analysis [13].

The deduced TOF were converted into mass values by fitting a polynomial function between the rest masses of the calibration nuclides [24] Mc^2 divided by $q = Z$ and the centers of gravity $TOF(Z, A)$, with their respective uncertainties.

$$\frac{Mc^2}{Z} = \alpha_0 + \alpha_1 TOF + \alpha_2 TOF^2 \quad (2)$$

The presence of quadratic terms in eq.2 arise from: (1) the relativistic factor which depends on TOF^2 ; (2) collection time differences in the silicon detectors and (3) the small energy losses in the foils of the micro-channel plate detectors. As these terms depend on Z , we expect a Z dependence of the expansion coefficients, however this explicit Z dependence could not be determined in our analysis given that only two Z values were transmitted per $B\rho_1$.

The calibration masses Mc^2 are defined as,

$$Mc^2 = A \cdot u + \Delta M - Z \cdot m_e c^2 \quad (3)$$

where $1u = 931.4940090(71)$ MeV is the atomic mass unit, ΔM are the calibration atomic mass excesses [24] and $m_e c^2 = 0.510998902(21)$ MeV is the rest mass

of the electron. The chosen reference masses were all those measured previously in at least two independent measurements with a precision that is much better than the best measurement made here. Below, we will discuss in detail the choice of calibration masses for each Z -value.

The quadratic expansion yielded a good fit with values of $\chi^2 \leq 1$ for a large part of the data. In three runs where the magnetic rigidity $B\rho_1$ used to select the secondary ions (when in $Z - 1$ charge state) was slightly different from the optimum value, as deduced from the measured rigidity $B\rho_2$ a small, higher order, cubic term was required to obtain a good fit. Given this additional complication, we decided not to include the data from these three runs in the final analysis. A systematic error of $3.5Z$ keV was added in quadrature with the statistical uncertainty for each mass and with the mass uncertainty in the calibration masses to reduce the χ^2 values: among 12 runs six had $\chi^2 < 1$, four had $1 < \chi^2 < 2$ and two had $2 < \chi^2 < 3$.

The determination of new masses for species not used as calibration references, was made by transforming the TOF into a mass value using the respective fit function. The uncertainty of these new masses was calculated by the quadratic combination of the systematic error, the statistical uncertainty and the extrapolation error obtained using the covariance matrix of the fit function. In table I we show the uncertainties of different sources: statistical, systematic and extrapolation, for the masses measured here. They are weighted mean values calculated over different runs for the same Z setting. We also list the total uncertainty as calculated from the quadratic sum.

In Fig. 2 we show the differences between our measured mass excess values and those from the AME'95 mass compilation [24]. As may be seen most of the results agree well with the tabulated values. In the following we discuss in detail the analysis performed, in particular for each Z -value.

III. RESULTS

A. Isomeric states

Several nuclei detected in our experiment have known isomeric states. They are presented in Table II, with the corresponding energies, half-lives, γ -decay energies and the isomeric ratios measured in this experiment using the germanium detectors. The isomeric ratio (F) is defined as

$$F = \frac{N_{isomer}}{N_{ion}} \quad (4)$$

where N_{isomer} is the total number of ions created in an isomeric state (at the production target) and N_{ion} is the total number of ions created of the same species.

N_{ion} is corrected for dead-time losses and N_{isomer} for in-flight losses as,

$$N_{isomer} = \frac{N_{\gamma}}{\epsilon e^{-\lambda TOF}} \quad (5)$$

where N_{γ} is the intensity of the γ -transition measured in the Ge-detector, ϵ the absolute efficiency of the Ge-detector at the γ -ray energy and $\lambda = \ln 2 / \gamma T_{1/2}$.

Strong isomeric transitions were observed for $^{67,69}\text{Ge}$, $^{69,71}\text{Se}$ as has been previously found [25,26] with γ -ray energies of 734, 398, 535 and 260 keV respectively (all transitions are $J^{\pi} = 9/2^{+} \rightarrow 5/2^{-}$). We also observed weak isomeric transitions ($E_{\gamma} = 394, 837$ keV) in ^{66}As [27]. Due to attenuation in the walls of the Si-telescope vacuum chamber, only γ -decaying isomeric transitions with energies higher than 100 keV could be observed. No corrections due to internal conversion were made.

The average mass-value $M_{gs} + \delta M$ was calculated by integrating over the TOF to account for in-flight decay of the isomer, whereby

$$\delta M = \frac{E_{\gamma} F}{\lambda TOF} (1 - e^{-\lambda TOF}). \quad (6)$$

The isomeric mass corrections δM are presented in Table II. The average mass-value $M_{gs} + \delta M$ was used as the reference mass for ^{67}Ge , ^{70}As , $^{69,73}\text{Se}$ and $^{72,74}\text{Br}$, where isomers were present. For the new mass measurements (^{69}Ge , ^{66}As and ^{71}Se) the isomeric contributions δM were subtracted from the measured masses before comparing them with Audi-Wapstra mass systematics (Tables II and III and Figure 2).

B. Reference masses

The isotopes of germanium observed here were $^{63-73}\text{Ge}$, with $^{67,68}\text{Ge}$ exhibiting the highest counting statistics while the most exotic isotope ^{63}Ge was observed as 20 events. The isotopes $^{66-68,70}\text{Ge}$ were chosen as calibration masses, with the mass excesses and uncertainties taken from Ref. [24]. The mass correction for ^{67}Ge due to isomeric states is given in Table II.

The isotopes of arsenic observed here were $^{65-75}\text{As}$ with $^{69,70}\text{As}$ exhibiting the highest counting statistics. Only 2 events were observed for ^{65}As . The masses of $^{69-72}\text{As}$ were used as reference masses. The masses of $^{69,71,72}\text{As}$ were taken from [24] and of ^{70}As from a recent mid-stream evaluation [28] performed with the inclusion of new experimental data which gave $\Delta M(^{70}\text{As}) = -64420(45)$ keV. The nucleus ^{70}As has a known isomeric state at 32 keV, but because of the low energy the γ -decay was not observed here. For this work we adopted a mass for ^{70}As which is the mean

value between the ground and isomeric state masses. The mass of ^{68}As was recently measured using the ESR storage ring at GSI [29]. The new mass excess value (-58890(100) keV) is in good agreement with a previous β -decay measurement [30] and value adopted in the latest mass evaluation [24] (-58880(100) keV). Thus, the mass value for ^{68}As which we used here as a reference was the average of these two results, $\Delta M = -58885(70)$ keV. By including ^{68}As as calibration mass, the extrapolation errors for $^{66,67}\text{As}$ could be reduced from 880 to 380 keV and from 510 to 200 keV, respectively.

The isotopes of selenium observed here were $^{67-77}\text{Se}$ with the most exotic isotope being the ^{67}Se with 8 events. The highest counting statistics were for $^{71,72}\text{Se}$. The reference masses used in the calibration were $^{69,72-74}\text{Se}$. The nucleus ^{69}Se has two isomeric states with half-lives longer than the TOF [25,26] and the corresponding isomeric mass correction is given in Table II. The isotope ^{73}Se has an isomeric state 26 keV above the ground-state with a half life of 39.80 m. As for ^{70}As mentioned above, we used a mean ground state - isomeric state mass value for ^{73}Se .

The isotopes of bromine observed here were $^{70-77}\text{Br}$ with the most exotic species being ^{70}Br for which some 58 events were collected. The reference masses were $^{72,73,74,75}\text{Br}$. For the ^{72}Br ground-state mass we adopted a weighted mean value of $\Delta M = -59040(90)$ keV, which is derived from the mass table [24] (-59150(260) keV) and a recent $\beta - \gamma$ coincidence measurement [31] (-59025(96) keV). For ^{73}Br the mid-stream evaluation [28] yielded $\Delta M = -63631(51)$ keV and was used as the calibration mass. Both ^{72}Br and ^{74}Br have known isomeric states (see Table II), but due to the low γ -ray energies the decays were not observed. The reference masses used were the mean values between the ground-state and isomeric masses. As may be seen from the uncertainties quoted on the masses here the uncertainty in the isomeric fractions have an insignificant influence on the final mass determinations.

C. New mass measurements

^{64}Ge

The present work yielded a mass for ^{64}Ge of $\Delta M = -53180(640)$ keV which is 1240(640) keV higher than the previous determination from a β^{+} -decay experiment [32]. Here the γ -spectrum in coincidence with ^{64}Ge exhibited a very low yield and no γ -ray peaks were observed. However, due to a low γ detection efficiency the population of an unknown isomeric state could not be excluded and only an upper limit of

$F \leq 34(34)\%$ could be established for $E^m \geq 300$ keV and $T_{1/2} \geq 1\mu s$.

We have also calculated the Q -value for proton capture $Q_p = \Delta M(^{64}\text{Ge}) + \Delta M(p) - \Delta M(^{65}\text{As})$ of ^{64}Ge using our mass excess for ^{64}Ge and the Audi-Wapstra mass systematics for $\Delta M(^{65}\text{As}) = -47060(390)\#$ keV. We obtained $Q_p = 1170(750)\#$ keV which indicates that ^{64}Ge is not likely to be a waiting-point at a 1.6σ level in the rp-process. This is in sharp contrast to the previous mass measurement [24] which yields a $Q_p = -70(450)\#$ keV that suggests ^{64}Ge is a waiting-point nucleus. The mass excesses calculated in the context of the macroscopic-microscopic finite-range droplet model (FRDM) of Möller, Nix, Myers and Swiatecki [33] yields a low positive value of $Q_p = 129$ keV.

^{65}Ge

The present direct measurement yielded a mass-excess for ^{65}Ge of $\Delta M = -55960(250)$ keV which is $450(250)$ keV larger than the mass quoted in the Audi-Wapstra tables [24]. The coincident γ -spectrum for ^{65}Ge , the yield for which was quite high ($N_{ion}=36750$) exhibited no lines. From this we can calculate for $E^m \geq 300\text{keV}$ and $T_{1/2} \geq 1\mu s$ an upper limit of $F \leq 2(1)\%$ and conclude that ^{65}Ge probably has no isomeric state that is appreciably populated. For a much shorter half-life ($T_{1/2} \geq 0.1\mu s$) the upper limit increases to 40%.

^{69}Ge

A strong 398 keV γ -transition was observed in coincidence with ^{69}Ge while no evidence was seen for the 89 keV transition (see Table II) due to attenuation by the walls of the vacuum chamber. An isomeric fraction of 100(2)% was determined for the 398 keV state of ^{69}Ge which yielded a mass correction of $\delta M = 362(9)$ keV (see eq. 6). The mass excess of ^{69}Ge determined in the present experiment is $410(120)$ keV above the ground-state mass excess obtained in earlier measurement, in good agreement with the isomeric correction of $362(9)$ keV. In Figure 2 this isomeric contribution was subtracted from the measured mass to allow comparison to be made with the Audi-Wapstra compilation.

In a recent paper [34] the isomeric ratio of nuclei produced in fragmentation reactions was studied. This work showed a strong dependence on the structure and spin of the isomer as well as the number of nucleons removed. In the fragmentation of a 60MeV/nucleon ^{92}Mo beam on a ^{27}Al target, the isomeric ratio for the 398 keV state in ^{69}Ge was measured to be 70(5)% [34].

The results of the mass determination for $^{64,65}\text{Ge}$ are displayed in Table III and Figure 2. In Table III the mass excesses calculated using the FRDM [33] are also presented. The masses for $^{64,65}\text{Ge}$ obtained in

the present work are less bound than the values cited in the Audi-Wapstra mass tables [24], but very close to the FRDM predictions. Comparison between Q_p values for the proton capture on ^{64}Ge can be found in Table IV.

^{66}As

Recent experiments have observed two isomeric states in ^{66}As at 1356.7 keV ($T_{1/2}=1.1(1)\mu s$) and 3023.9 keV ($T_{1/2}=8.2(5)\mu s$) [27]. While the strongest γ -transitions from the 1356.7 keV isomeric state (394, 837 and 964 keV) could be observed in our experiment, the transitions de-exciting the 3023.9 keV isomeric state were not observed. From our measurements we estimate that the isomeric fraction for the $E^m = 1356.7$ keV isomeric state is $F = 35(17)\%$. This results in an isomeric mass correction of $476(200)$ keV. After subtracting this contribution, a ^{66}As mass excess of $\Delta M = -51500(680)$ keV was obtained, some 320 keV above the adopted ground-state mass excess [24]. The mass of ^{66}As was previously measured in a β -decay experiment [35], yielding $\Delta M = -52070$ keV. This value however, was not included in the latest mass evaluation due to its discrepancy with expected S_{2n} value. Our result, although not very precise, tends to confirm this choice.

^{67}As

The mass of ^{67}As was previously reported with an uncertainty of 100 keV [36]. Our measured mass-excess of $\Delta M = -56360(240)$ keV is $280(240)$ keV above the adopted value. For $^{66,67}\text{As}$ the FRDM masses are again less bound than the masses quoted in the Audi-Wapstra tables. The masses derived from the present measurements are, however, closer to the Audi-Wapstra systematics.

^{68}Se

The γ -ray spectrum in coincidence with ^{68}Se exhibited very low statistics with no visible lines. Owing to the low flux of ^{68}Se and reduced γ -detection efficiency, the presence of isomeric states could not be excluded. One can establish for $E^m \geq 300$ keV and $T_{1/2} \geq 1\mu s$, an isomeric fraction limit of $F \leq 23(23)\%$. There is no limit for F if the half-life is much shorter ($T_{1/2} \geq 0.1\mu s$).

The present work finds a mass excess for ^{68}Se of $\Delta M = -53620(1000)$ keV, which is within in a standard deviation of the Audi-Wapstra extrapolated value of $-54150\#$ keV [24] and the FRDM prediction of $\Delta M = -53550$ keV [33].

^{70}Se

As given in Table III our measurement for ^{70}Se yields a mass excess of $-61960(130)$ keV. This agrees with recent measurements of $-61604(100)$ keV by Tomlin et al. [31] using β - γ coincidence spectroscopy and $-62070(70)$ keV by Hausmann et al. [29] using the ESR

storage ring, as well as our previously published result from the same data set of -62310(460) keV [13].

⁷¹Se

The nucleus ⁷¹Se has a 9/2⁺ isomeric state at 260 keV which decays with a half life of 27.4 μ s [25]. A strong 260 keV γ -transition was observed in the present experiment and an isomeric fraction of $F = 22(1)\%$ was determined. The mass correction due to the isomeric state was 58(2) keV. The mass excess after accounting for the isomeric correction was $\Delta M(^{71}\text{Se}) = -63180(110)$ keV which is in good agreement with earlier measurements (-63130(35) [31] and -63050(70) keV [29]) and our previous result of -63490(320) keV using the same data set [13].

⁶⁹Br

This nucleus, which has been suggested to be proton unbound by at least 500 keV [9,23], was not observed in our measurements. The mass excess has been estimated to be $\Delta M(^{69}\text{Br}) = -46410(310)\#$ keV [24]. Using our mass for ⁶⁸Se we obtain a $Q_p(^{68}\text{Se}) = \Delta M(^{68}\text{Se}) + \Delta M(\text{p}) - \Delta M(^{69}\text{Br}) = 80 \pm 1030\#$ keV. Given the large uncertainty this result is compatible with ⁶⁹Br being proton unbound and with ⁶⁸Se acting as a waiting-point. Comparison between the Q_p values for proton capture on ⁶⁸Se for different estimates of the masses can be found in Table IV.

⁷¹Br

Some 2200 events were observed for this nucleus. As listed in table III the present measurement of ⁷¹Br yielded a mass excess of -57060(570) keV, in agreement within uncertainties with the Audi-Wapstra systematics [24] and the FRDM prediction [33].

IV. CONCLUSIONS

The very neutron-deficient nuclei ^{62,63}Ge, ⁶⁵As, ⁶⁷Se and ⁷⁰Br were observed, confirming their particle stability, but with statistics that were too poor to report a reliable mass. No events for ⁶⁹Br were observed consistent with previous experiments claiming it to be unbound. The masses of ⁶⁶As, ⁶⁸Se and ⁷¹Br were determined in the present experiment with uncertainties of between 570 and 1000 keV (Table III). The mass of ⁶⁸Se was found to be compatible with ⁶⁹Br being unbound and suggests that ⁶⁸Se be a waiting point in the rp-process. These encouraging results will be confirmed in the future by repeating this measurement at GANIL with better statistics.

The masses obtained for ^{70,71}Se are in good agreement with recent measurements and are of comparable precision. The masses of ^{64,65}Ge and ⁶⁷As are reported with uncertainties of 200 to 600 keV. The result for ⁶⁴Ge is 1240(640) keV less bound than previous measurement [24] and suggests that ⁶⁴Ge is not a waiting-point in the rp-process.

The measured masses of ^{64,65}Ge, ⁶⁸Se and ⁷¹Br are in good agreement with the predictions of the macroscopic-microscopic FRDM model [33]. The measurement of γ -rays in coincidence with ions of interest allowed the presence of isomers to be identified and the populations to be derived. The masses were subsequently corrected to account for this. Importantly this improved the precision in the masses used for ⁶⁷Ge and ⁶⁹Se which served as references. In the case of ⁶⁹Ge the isomeric mass correction ($\delta M = 362(9)$ keV) determined from γ -ray data provided a mass in very good agreement with the known value.

Acknowledgements

G.F.L, R.L. and A.L-Sz. wish to thank the Fundação ao Amparo de Pesquisa do Estado de São Paulo (FAPESP) and the Conselho Nacional de Desenvolvimento Tecnológico e Científico (CNPq) for financial support. The assistance of the SPEG crew (J. F. Libin and P. Gagnant) in setting up the experiment is also fully acknowledged.

-
- [1] R. Wallace and S. E. Woosley, *Astrophys. J. Suppl.* **45**, 309 (1981).
 - [2] L. Van Wormer *et al.* *Astrophys. J.* **432**, 326 (1994).
 - [3] S. E. Woosley and T. A. Weaver, in *High Energy Transients in Astrophysics*, Vol.115 of *AIP Conference Proceedings*, ed. S. E. Woosley (AIP, New York,1984) p. 273.
 - [4] H. Schatz *et al.*, *Phys. Reports R.* **294**, 167 (1998).
 - [5] M. Mohar *et al.*, *Phys. Rev. Lett.* **66**, 1571 (1991).
 - [6] S. J. Yennello *et al.*, *Phys. Rev.* **C46**, 2620 (1992).
 - [7] J. C. Batcheler *et al.*, *Phys. Rev.* **C47**, 2038 (1993).
 - [8] J. A. Winger *et al.*, *Phys. Lett.* **B299**, 214 (1993).
 - [9] B. Blank *et al.*, *Phys. Rev. Lett.* **74**, 4611 (1995).
 - [10] P. Van Isacker and D. D. Warner *Phys. Rev. Lett.* **78**, 3266 (1997).
 - [11] D. S. Brenner, C. Wesselborg, R. F. Casten, D. D. Warner and J. Y. Zhang *Phys. Lett.* **B243**, 1 (1990).
 - [12] P. Van Isacker, D. D. Warner and D. S. Brenner *Phys. Rev. Lett.* **74**, 4607 (1995).
 - [13] M. Chartier *et al.*, *Nucl. Phys.* **A637**, 3 (1998).
 - [14] A. Gillibert *et al.*, *Phys. Lett.* **B192**, 39 (1987).
 - [15] N. A. Orr *et al.*, *Phys. Lett.* **B258**, 29 (1991).
 - [16] F. Sarazin *et al.*, *Phys. Rev. Lett.* **84**, 5062 (2000).
 - [17] A. Joubert, *Proc. 1991 Particle Accelerator Conference, IEEE*, 1 (1991).
 - [18] L. Bianchi *et al.*, *Nucl. Instr. Meth.* **A276**, 509 (1989).
 - [19] O. H. Odland *et al.*, *Nucl. Instr. Meth.* **A378**, 149 (1996).
 - [20] J. A. Winger, B. M. Sherrill and D. J. Morrissey *Nucl. Instr. Meth.* **B70**, 380 (1992).
 - [21] D. Bazin and O. Sorlin, <http://www.nscl.msu.edu/bazin/LISE.html>.

- [22] W. Mittig *et al.*, Nucl. Phys. **A616**, 329 (1997).
 [23] R. Pfaff *et al.*, Phys. Rev. **C53**, 1573 (1996).
 [24] G. Audi and A. H. Wapstra, Nucl. Phys. **A595**, 409 (1995).
 [25] C. Chandler *et al.*, Phys. Rev. **C61**, 044309 (2000).
 [26] K. R. Pohl *et al.*, Phys. Rev. **C51**, 519 (1995).
 [27] R. Grzywacz *et al.*, Nucl. Phys. **A682**, 41c (2001).
 [28] A. H. Wapstra and G. Audi, priv. comm. june 2001.
 [29] M. Hausmann *et al.*, Hyp. Inter. **132**, 289, 2001.
 [30] R. C. Pardo *et al.*, Phys. Rev. **C15**, 1811 (1977).
 [31] B. E. Tomlin *et al.*, Phys. Rev. **C63**, 034314 (2001).
 [32] C. N. Davids and D. R. Goosman, Phys. Rev. **C7**, 122 (1973).
 [33] P. Möller, J. R. Nix, W. D. Myers and W. J. Swiatecki Atom. Data and Nucl. Data Tables **59**, 185 (1995).
 [34] J. M. Daugas *et al.*, Phys. Rev. **C63**, 064609 (2001).
 [35] C. N. Davids, Proc. 6th Int. Conf. on Atomic Masses and Fund. Constants (AMCO-6), East Lansing, 1979, p.419.
 [36] M. J. Murphy *et al.*, Phys. Rev. **C22**, 2204 (1980).

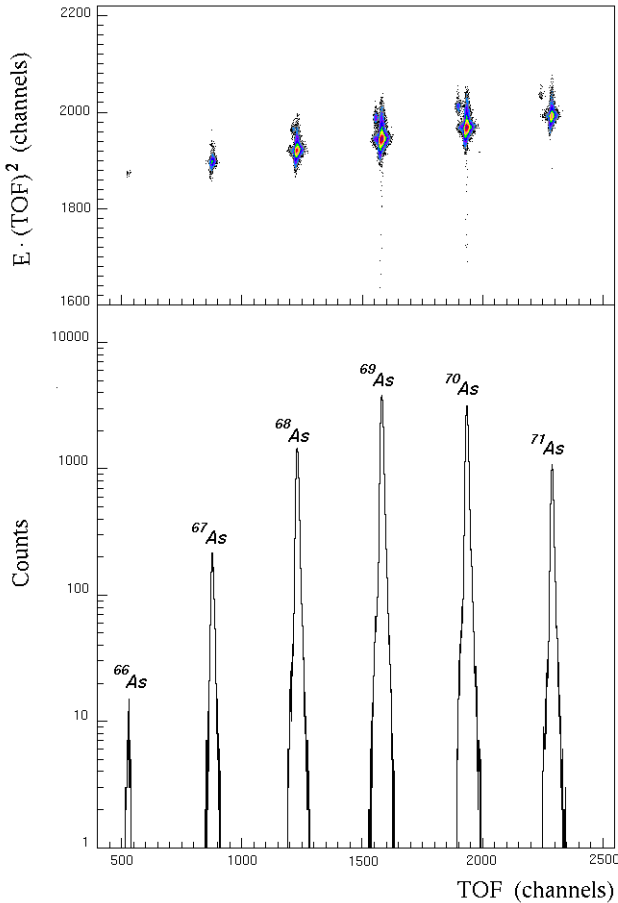


FIG. 1. Upper panel: Two-dimensional spectrum displaying the isotopes present in the ${}_{33}\text{As}$ chain. Note the neighbouring elements that appear as contaminants (see text). Lower panel: Projection of the isotopes of interest on the TOF axis.

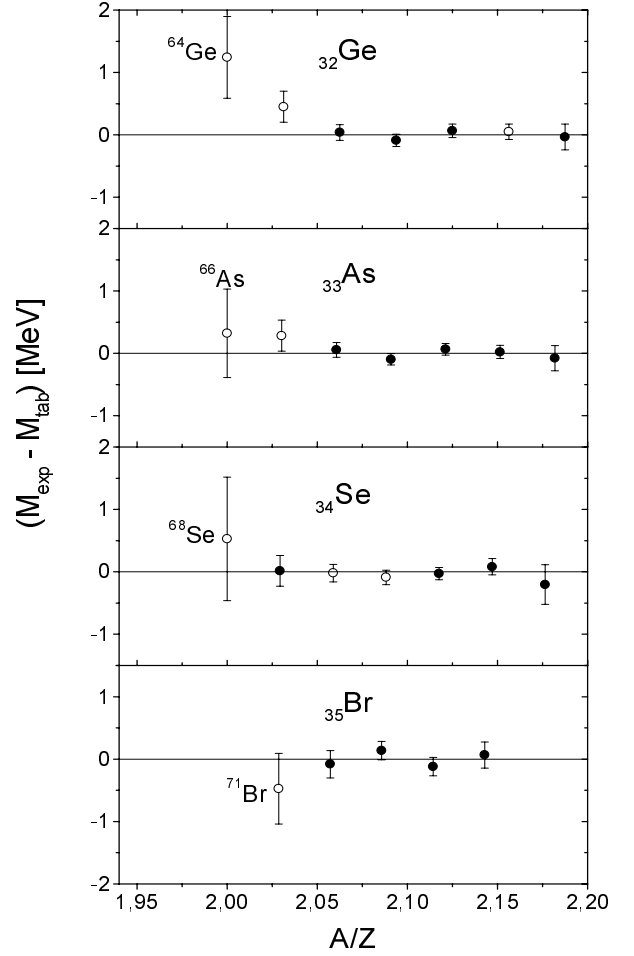


FIG. 2. Comparison of present mass values M_{exp} and those of the Audi-Wapstra table M_{tab} [24]. The isotopes which were used as reference masses are indicated by the filled circles and the new masses by open circles. Isomeric contributions were taken into account as described in the text.

| Nuclide | σ_{stat} (keV) | σ_{sys} (keV) | σ_{extr} (keV) | σ_{tot} (keV) | δM (keV) |
|--------------------|--------------------------|-------------------------|--------------------------|-------------------------|---------------------|
| ${}^{64}\text{Ge}$ | 490 | 80 | 390 | 640 | - |
| ${}^{65}\text{Ge}$ | 100 | 80 | 210 | 250 | - |
| ${}^{69}\text{Ge}$ | 44 | 80 | 80 | 120 | 362(9) |
| ${}^{66}\text{As}$ | 530 | 70 | 380 | 650 | 476(200) |
| ${}^{67}\text{As}$ | 110 | 66 | 200 | 240 | - |
| ${}^{68}\text{Se}$ | 940 | 50 | 300 | 1000 | - |
| ${}^{70}\text{Se}$ | 60 | 50 | 110 | 130 | - |
| ${}^{71}\text{Se}$ | 40 | 50 | 90 | 110 | 58(2) |
| ${}^{71}\text{Br}$ | 360 | 90 | 430 | 570 | - |

TABLE I. Contributions from different sources to the final uncertainty (tot): statistical (stat), systematic (sys) and extrapolation (extr). The isomeric mass corrections are listed in the last column.

| Nuclide | E^m (keV) | E_{γ}^{obs} (keV) | $T_{1/2}$ (μ s) | F(%) | δM (keV) |
|-------------|----------------|-----------------------------|-------------------------|--------|---------------------|
| $^{67}Ge^*$ | 18(5) | - | 13.7 | - | - |
| $^{67}Ge^*$ | 752(6) | 734 | 0.146 | 7(2) | 17(4) |
| ^{69}Ge | 86.76 | - | 5.1 | - | - |
| ^{69}Ge | 397.95 | 398 | 2.81 | 100(2) | 362(9) |
| ^{66}As | 1356.7 | 394 | 1.1 | 35(17) | 476(200) |
| ^{66}As | 1356.7 | 837 | 1.1 | 35(17) | 476(200) |
| $^{70}As^*$ | 32.06 | - | 96 | 50 | 16 |
| $^{69}Se^*$ | 39.4 | - | 2.0 | - | - |
| $^{69}Se^*$ | 573.9 | 534.5 | 1.37 | 29(4) | 140(20) |
| ^{71}Se | 260.48 | 260.5 | 27.4 | 22(1) | 58(2) |
| $^{73}Se^*$ | 25.71 | - | 39.8m | 50 | 13(4) |
| $^{72}Br^*$ | 100.92 | - | 10.6s | 50 | 50(30) |
| $^{74}Br^*$ | 13.58 | - | 46m | 50 | 7(4) |

TABLE II. Isomeric states detected in this experiment. Reference masses (indicated by *) were corrected for the isomeric state contribution δM . The column $F(\%)$ lists the fractional population of the isomer (see text).

| | This work | ISO-ESR | β -decay | AME'95+[27] | FRDM |
|-----------|--------------|------------|----------------|--------------|--------|
| ^{64}Ge | -53180(640) | - | - | -54420(250) | -53040 |
| ^{65}Ge | -55960(250) | - | - | -56410(100) | -55580 |
| ^{66}As | -51500(680) | - | -52070(50) | -51820(200)# | -49970 |
| ^{67}As | -56360(240) | - | - | -56650(100) | -55960 |
| ^{68}Se | -53620(1000) | - | - | -54150(300)# | -53550 |
| ^{70}Se | -61960(130) | -62070(70) | -61604(100) | -61940(210)# | -61870 |
| ^{71}Se | -63180(110) | -63050(70) | -63130(35) | -63090(200)# | -63390 |
| ^{71}Br | -57060(570) | - | - | -56590(300)# | -56790 |

TABLE III. Comparison between the mass excesses obtained in the present work (keV) with recent results and predictions: ISO-ESR[29], β -decay[31,35], Audi-Wapstra (AME'95[24] and [28]) and FRDM [33]. A previous analysis of the same data set yielded $\Delta M(^{70}Se) = -62310(460)$ keV and $\Delta M(^{71}Se) = -63490(320)$ keV [13].

| Nuclide | Q_p (this work) (keV) | Q_p (A-W) (keV) | Q_p (FRDM) (keV) |
|-----------|----------------------------|----------------------|-----------------------|
| ^{64}Ge | 1170(750) | -70(450) | 129 |
| ^{68}Se | 80(1030) | -450(430) | 89 |

TABLE IV. Comparison between Q_p derived from the present work and those of Audi-Wapstra [24] and from FRDM calculations[33]. The Q_p were calculated as $Q_p(Z, N) = \Delta M(Z, N) + \Delta M(p) - \Delta M(Z + 1, N)$. The Audi-Wapstra estimations for ^{65}As (-47060(390)# keV) and for ^{69}Br (-46410(310)# keV) were used.